



Speciation and sorption structure of diphenylarsinic acid in soil clay mineral fractions using sequential extraction and EXAFS spectroscopy

Meng Zhu^{1,3,4} · Xuefeng Hu³ · Chen Tu³ · Yongming Luo^{2,3} · Ruyi Yang^{1,4} · Shoubiao Zhou^{1,4} · Nannan Cheng¹ · Elizabeth L. Rylott⁵

Received: 22 May 2019 / Accepted: 6 August 2019 / Published online: 13 August 2019
© Springer-Verlag GmbH Germany, part of Springer Nature 2019

Abstract

Purpose The mobility of arsenic (As) in soils is fundamentally affected by the clay mineral fraction and its composition. Diphenylarsinic acid (DPAA) is an organoarsenic contaminant derived from chemical warfare agents. Understanding how DPAA interacts with soil clay mineral fractions will enhance understanding of the mobility and transformation of DPAA in the soil-water environment. The objective of this study was to investigate the speciation and sorption structure of DPAA in the clay mineral fractions.

Materials and methods Twelve soils were collected from nine Chinese cities which known as chemical weapons burial sites and artificially contaminated with DPAA. A sequential extraction procedure (SEP) was employed to elucidate the speciation of DPAA in the clay mineral fractions of soils. Pearson's correlation analysis was used to derive the relationship between DPAA sorption and the selected physicochemical properties of the clay mineral fractions. Extended X-ray absorption fine structure (EXAFS) L_{III}-edge As was measured using the beamline BL14W1 at Shanghai Synchrotron Radiation Facility (SSRF) to identify the coordination environment of DPAA in clay mineral fractions.

Results and discussion The SEP results showed that DPAA predominantly existed as specifically fraction (18.3–52.8%). A considerable amount of DPAA was also released from non-specifically fraction (8.2–46.7%) and the dissolution of amorphous, poorly crystalline, and well-crystallized Fe/Al (hydr)oxides (20.1–46.2%). A combination of Pearson's correlation analysis and SEP study demonstrated that amorphous and poorly crystalline Fe (hydr)oxides contributed most to DPAA sorption in the clay mineral fractions of soils. The EXAFS results further demonstrated that DPAA formed inner-sphere complexes on Fe (hydr)oxides, with As-Fe distances of 3.18–3.25 Å. It is likely that the steric hindrance caused by phenyl substitution and hence the instability of DPAA/Fe complexes explain why a substantial amount of DPAA presented as weakly bound forms.

Conclusions DPAA in clay mineral fractions predominantly existed as specifically, amorphous, poorly crystalline, and crystallized Fe/Al (hydr)oxides associated fractions. Amorphous/poorly crystalline Fe rather than total Fe contributed more to DPAA sorption and DPAA formed inner-sphere complexes on Fe (hydr)oxides.

Responsible editor: Zhaohui Wang

Electronic supplementary material The online version of this article (<https://doi.org/10.1007/s11368-019-02431-2>) contains supplementary material, which is available to authorized users.

✉ Yongming Luo
ymluo@yic.ac.cn

¹ College of Environmental Science and Engineering, Anhui Normal University, Wuhu 241002, People's Republic of China

² Key Laboratory of Soil Environment and Pollution Remediation, Institute of Soil Science, Chinese Academy of Sciences, Nanjing 210008, People's Republic of China

³ Key Laboratory of Coastal Environmental Processes and Ecological Remediation, Yantai Institute of Coastal Zone Research, Chinese Academy of Sciences, Yantai 264003, People's Republic of China

⁴ Anhui Provincial Engineering Laboratory of Water and Soil Pollution Control and Remediation, Anhui Normal University, Wuhu 241002, People's Republic of China

⁵ Centre for Novel Agricultural Products, Department of Biology, University of York, York YO10 5DD, UK

Keywords Diphenylarsinic acid (DPAA) · EXAFS · Sequential extraction · Speciation · Sorption structure

1 Introduction

Clark I (diphenylchloroarsine) and Clark II (diphenylcyanoarsine) were widely produced during World Wars I and II as chemical warfare agents. Subsequently, these agents were disposed of in China, Europe, and Japan primarily by earth-burying and sea-dumping (Deng and Evans 1997; Garnaga et al. 2006; Daus et al. 2010). Leaching of diphenylarsinic acid (DPAA) (Fig. S1, Electronic Supplementary Material—ESM), a degradation product of Clark I and Clark II, from munitions to soil and from soil to groundwater has gained increasing attention (Hanaoka et al. 2005a, b) due to its high persistence in the soil-water environment (Hempel et al. 2009); a factor exacerbated by its high bioaccessibility (Arao et al. 2009) and mobility (Maejima et al. 2011), as well as its high cytotoxic and genotoxic effects (Ochi et al. 2004). To evaluate the potential environmental and health risks of DPAA, it is essential to fully understand its sorption behavior and mobility in soils. A study indicates that DPAA is specifically adsorbed onto soil minerals rather than by hydrophobic interaction with soil organic matter (SOM) (Maejima et al. 2011), and Fe (hydr)oxide is understood to be the primary component responsible for DPAA sorption in soil (Wang et al. 2013), but no direct evidence has been provided. More chemical and molecular information are still urgently required to elucidate the interactions between DPAA and soil minerals.

Sequential extraction procedure (SEP) has been applied for a long time to characterize the interactions of arsenic (As) with soil minerals, and the following speciations of As are determined: non-specifically sorbed, specifically sorbed, amorphous and poorly crystalline Fe/Al (hydr)oxides associated, well-crystallized Fe/Al (hydr)oxides associated, and residual phases (Girouard and Zagury 2009; Wang et al. 2015). van Herreweghe et al. (2003) used a SEP to extract As from industrially contaminated soils and found that the majority of As was released after NaOH extraction; this fraction accounts for As bound to the surface of Fe-rich minerals according to Manful (1992). Although SEP is a relatively simple method to determine As speciation, several constraints to this technique have been reported, such as limited precision, selectivity, and redistribution of analytes among phases during extraction (Bacon and Davidson 2008; Wang and Mulligan 2008). Most importantly, SEP results should be considered only in operational defined fractions; it provides no information relevant to the sorption structure of As. To overcome these limitations, it is necessary to combine SEP with other characterization techniques.

Extended X-ray absorption fine structure (EXAFS) spectroscopy is a powerful technique that directly determines

chemically bound forms and local coordination environment of As in soils. Arçon et al. (2005) identified that, in a contaminated soil, Fe and Al atoms occurred in the next neighbor coordination shells around As, with an As-Fe distance at 3.34 Å and As-Al distance at 2.54 Å, suggesting that As was mainly present as Fe- and Al-bound forms. Cancès et al. (2005) used EXAFS to investigate an As-contaminated soil from a former pesticide plant. They observed that 0.7–1.9 Fe atoms were located at As-Fe distances of ca. 3.3 Å, corresponding to As linked to Fe (hydr)oxides by double-cornering sharing. However, although considerable EXAFS work has been devoted to study the coordination environment of inorganic As in soil, much less is known for organoarsenic compounds.

The molecular environment of organoarsenic compounds in the soil environment is primarily provided by their interactions with Fe (hydr)oxides (Fu et al. 2016). Shimizu et al. (2011) investigated the sorption structure of monomethylarsenate (MMA) and dimethylarsenate (DMA) on goethite and found that both compounds formed bidentate binuclear cornering sharing (2C) bonds. Tanaka et al. (2014) observed that both DPAA and phenylarsinic acid (PAA) (Fig. S1—ESM) formed 2C and monodentate mononuclear corner-sharing (1V) bonds on ferrihydrite. More recently, we identified both inner-sphere 2C complexes and out-sphere complexes for DPAA sorption on ferrihydrite, goethite and hematite (Zhu et al. 2019). However, no EXAFS work has been devoted to the sorption of DPAA, and other phenyl arsenic compounds, to soil, which may be due to the weak retention of these compounds, and thus low signal value and high background noise.

The majority of active sites responsible for As sorption in soils are in the clay mineral fractions (< 2- μ m diameter) (Lombi et al. 2000). Their increased retention of As compared with the whole soil will ease the application of EXAFS technique. Thus, by using these fractions, the problems of low signal and high background noise could be overcome, making this a good model to use EXAFS. The objective of this study was to determine the specific speciation and local coordination environment of DPAA in clay mineral fractions using a combination of SEP and EXAFS techniques. The SEP and EXAFS data in this study is compared with the available literature data of inorganic, methyl, and phenyl arsenics and discussed in terms of group substitution. The results deepen our understanding in the sorption, partitioning, and mobility of DPAA and also throw lights on risk assessment and the development of remediation strategies for DPAA in the soil-water environment.

2 Materials and methods

2.1 Soil samples and clay mineral fraction isolation

Twelve soils were collected from nine Chinese cities where chemical weapons burial sites have been found according to Deng and Evans (1997). The soil types were classified according to Gong (2007). Soil properties were analyzed mainly according to the methods of Lu (2000). Briefly, soil pH was determined in soil/water ratio 1:2.5. Cation exchange capacity (CEC) was measured using sodium acetate–ammonium acetate extraction. Point of zero charge (PZC) was analyzed using salt titration method (Sakurai et al. 1988). SOM was measured using dichromate oxidation. Fe was extracted using dithionite-citrate-bicarbonate (DCB), ammonium oxalate, and HF-HNO₃-HClO₄ solutions separately (Pretorius et al. 2006), representative of the free Fe forms (Fe₂O_{3DCB}) consisting of both crystalline and non-crystalline Fe oxides, the amorphous and poorly crystalline Fe oxides (Fe₂O_{3oxalate}), and the total Fe (Fe_{total}), respectively. The extracted Fe was analyzed using *o*-phenanthroline photometric method. Al was extracted using DCB and HF-HNO₃-HClO₄ solutions separately, representative of the free Al oxides (Al₂O_{3DCB}) and the total Al (Al_{total}), respectively. The extracted Al was measured by inductively coupled plasma-optical emission spectroscopy (ICP-OES, Optima 7000 DV, Perkin Elmer Co., USA). Si extracted by HF-HNO₃-HClO₄ solution (Si_{total}) was also determined by ICP-OES. Soil particle composition was determined by a laser particle analyzer (Malvern Mastersizer 2000F, Malvern Instruments Ltd., UK). The concentrations of total As in soils were determined using atomic fluorescence spectrometry (AFS-930, Beijing Jitian Instrument Co., China) after HCl-HNO₃ digestion (GB/T 22105.2-2008).

All soil samples were air dried and sieved to obtain a particle size ≤ 2-mm diameter, then treated repeatedly with H₂O₂ according to Zhang and Gong (2012) until all organic matter was completely removed. Briefly, 30 g of soil was placed in a 1 L tall beaker and 300 mL of 30% H₂O₂-H₂O (v/v = 1:1) was added. The reaction was allowed to proceed at room temperature overnight and then at 60–70 °C in an electric stove. The treatment was repeated until no visible reaction could be detected by addition of more H₂O₂. The clay mineral fractions were then obtained by sedimentation after removing carbonate (Jackson 1975). To remove extra HCl introduced in carbonate elimination step, the clay mineral fraction was washed with ultra-pure water and freeze-dried before the sorption experiment. Selected physicochemical properties of the whole soils and their clay mineral fractions are presented in Table S1 (ESM) and Table 1, respectively. The mineralogy of the clay mineral fractions was verified by X-ray diffraction (XRD, Ultima IV, Rigaku) and the results are listed in Table S2 (ESM).

2.2 DPAA sorption

A DPAA solution (100 mg L⁻¹) was prepared in 0.01 mol L⁻¹ NaNO₃ as the background solution. The sorption experiments were carried out using a sorbent concentration of 50 g L⁻¹ in 50-mL Teflon tubes and performed in triplicate. The pH was adjusted to 6.0 with a 0.1 mol L⁻¹ HNO₃ or NaOH solution. All tubes were shaken at 150 rev min⁻¹ for 24 h at 25 ± 1 °C in the dark. Solids were harvested by centrifugation at 3000 rev min⁻¹ for 10 min. Two parallels were subjected directly to SEP analysis and one parallel was rinsed carefully with 0.01 mol L⁻¹ NaNO₃ to remove DPAA solution remaining in the sample; the wet paste, sealed in tubes, was used for EXAFS analysis.

2.3 Sequential extraction procedure

A five-step (i to v) SEP modified from Wenzel et al. (2001) was adopted for this study. In order to avoid DPAA oxidation, HNO₃-HCl instead of HNO₃-H₂O₂ was employed to extract residual DPAA. Step i, non-specifically sorbed DPAA was extracted with 0.05 mol L⁻¹ (NH₄)₂SO₄; step ii, specifically sorbed DPAA was extracted using 0.05 mol L⁻¹ (NH₄)₂HPO₄; step iii, DPAA associated with amorphous and poorly-crystalline Fe/Al (hydr)oxides was extracted using a 0.2 mol L⁻¹ NH₄-oxalate buffer (pH 3.25); step iv, DPAA bound to the well-crystallized Fe/Al (hydr)oxides was extracted using 0.2 mol L⁻¹ NH₄-oxalate and 0.1 mol L⁻¹ ascorbic acid (pH 3.25) and step v, residual DPAA was dissolved using HNO₃-HCl (v/v = 1:1). Following these steps, two additional wash steps were performed using NH₄-oxalate to remove residual DPAA from the solution, as described by Wenzel et al. (2001). Extracts from each step were analyzed for DPAA content using a high-performance liquid chromatography coupled with tandem mass spectrometry (HPLC-MS/MS) method with low matrix effect (102–107%), detection limit (0.01 µg L⁻¹), and intraday and interday previsions (< 5%) (Zhu et al. 2016a). The amount of DPAA sorbed (Q_{ads} , mg kg⁻¹ dry clay mineral fractions) was calculated as the sum of the DPAA extracted in the five-step SEP.

2.4 EXAFS data collection and analysis

Only four types of clay mineral fractions were selected for a detailed EXAFS analysis due to limited synchrotron time availability. All slurry samples were mounted in Kapton tape, then tightly sealed. The EXAFS data were collected at Shanghai Synchrotron Radiation Facility (SSRF) using the beamline BL14W1 equipped with a Si(111) double-crystal monochromator. During the measurement, the synchrotron was operated at energy of 3.5 GeV and 150 to 200 mA. All spectra were collected in fluorescence mode with 32-element Ge semiconductor detector, from -150 to 800 eV relative to

Table 1 The selected physicochemical properties of soil clay mineral fractions

Soil	Location	pH	PZC	CEC (cmol kg ⁻¹)	Fe ₂ O ₃ DCB (g kg ⁻¹)	Fe ₂ O ₃ oxalate (g kg ⁻¹)	Al ₂ O ₃ DCB (g kg ⁻¹)	Fe _{total} (g kg ⁻¹)	Al _{total} (g kg ⁻¹)	Si _{total} (g kg ⁻¹)
Orthic Acrisol	Yingtian, Jiangxi	4.01	4.04	27.13	89.29	5.89	31.92	78.36	120.12	3.60
Gleyic Acrisol	Yingtian, Jiangxi	4.84	3.66	35.70	49.90	6.56	30.71	56.38	127.11	3.03
Andosol	Beihai, Guangxi	6.32	5.71	24.75	144.69	7.80	41.05	122.59	145.89	2.99
Latosol-1	Wenchang, Hainan	5.84	4.10	0.14	156.34	1.90	51.31	121.23	137.39	2.91
Latosol-2	Wenchang, Hainan	5.56	4.31	22.30	138.68	3.91	37.98	127.16	171.71	3.29
Sulfic Aquic-Orthic Halosol	Haikou, Hainan	4.51	3.10	32.63	59.43	28.34	18.89	69.47	126.39	3.15
Latosolic soil	Dingan, Hainan	3.95	3.10	25.80	26.08	2.73	15.15	67.50	131.92	3.77
Brown soil-1	Dalian, Liaoning	4.43	3.34	40.25	23.64	2.54	30.57	75.41	122.33	2.90
Fluvo-aquic soil	Binzhou, Shandong	4.42	3.33	56.78	17.11	2.45	21.43	72.42	175.54	3.02
Brown soil-2	Yantai, Shandong	4.25	3.16	58.07	13.96	3.22	24.99	60.49	166.05	1.96
Phaeozem-1	Changchun, Jilin	4.85	3.51	49.50	20.73	10.81	32.06	75.68	120.55	2.96
Phaeozem-2	Changchun, Jilin	4.01	3.67	61.43	11.30	7.05	33.09	78.11	132.77	3.17

the As-K edge of 11,867 eV. Each EXAFS spectrum represented the average of three scans and each scan took 30–60 min to collect depending on exposure time. The obtained EXAFS spectra were analyzed using Artemis from the IFEFFIT software package (Newville 2001) and the procedure detailed in Zhu et al. (2019). Briefly, the EXAFS data were first background subtracted, averaged, normalized, and Fourier transformed, then back-transformed and fitted with the predicted function in which the coordination numbers (CN), their distances (R), Debye-Waller (σ^2), and threshold energies (ΔE_0) were varied to give the best fit. The *R* factor, which is defined as the mean square difference between the fit and the data on a point-by-point basis, was also reported and the value less than 0.05 accepted as a reasonable fit (Kelly et al. 2008).

2.5 Statistical analysis

Pearson's correlation analysis was used to derive the relationship between DPAA sorption and the selected physicochemical properties of the clay mineral fractions. SPSS version 20.0 was used to perform the Pearson's correlation analysis.

3 Results and discussion

3.1 Correlation between DPAA sorption and properties of clay mineral fractions

The level of sorption of DPAA on clay mineral fractions from the 12 soil types is shown in Fig. 1. All clay mineral fractions studied had sorbed significant amounts of DPAA after 24 h equilibration (Fig. 1). Pearson's correlation matrix on the physicochemical properties of clay mineral fractions and

DPAA sorption is listed in Table 2. It can be seen that the correlation coefficient between Q_{ads} and Fe_{total} was negative ($r = -0.190$) (Table 2), which is contrary to the previous observation that Acrisol soil had a stronger sorption capacity toward DPAA than Phaeozem soil due to its higher content of Fe (Wang et al. 2013). The results show that the total Fe content was not the key factor determining DPAA sorption in clay mineral fractions. A substantially higher positive correlation between Q_{ads} and $\text{Fe}_2\text{O}_{3\text{oxalate}}$ ($r = 0.440$) (Table 2) indicates that amorphous and poorly crystalline Fe (hydr)oxides could contribute more to DPAA sorption. This finding provides evidence of the importance of Fe speciation, rather than the total Fe content for DPAA sorption in clay mineral fractions. Similar results have been found for inorganic As (Palumbo-Roe et al. 2015). The Q_{ads} was also found to be positively correlated with CEC ($r = 0.354$, $p > 0.05$) (Table 2), suggesting that not only coordination mechanisms but also electrostatic attraction as well as interactions with Al_2O_3 or aluminosilicate could contribute to DPAA sorption in clay mineral fractions. The coexistence of multiple sorption mechanisms also has been reported for roxarsone, *p*-arsanilic acid (*p*AsA) (Fig. S1—ESM) and PAA sorption on soils (Arroyo-Abad et al. 2011) and may thereby explain the reduced Pearson correlation between Q_{ads} and $\text{Fe}_2\text{O}_{3\text{oxalate}}$.

3.2 DPAA speciation in clay mineral fractions

The results for solid phase speciation of DPAA using a SEP are shown in Fig. 1. The percentage difference between the total recovery (the sum of the five-step SEP) and the expected value (the total amount obtained by sorption experiment) was systematically lower than 13%. This deviation justifies the use of this SEP method. The non-specifically fraction (step i) constituted less than 30% of the total DPAA in the clay mineral

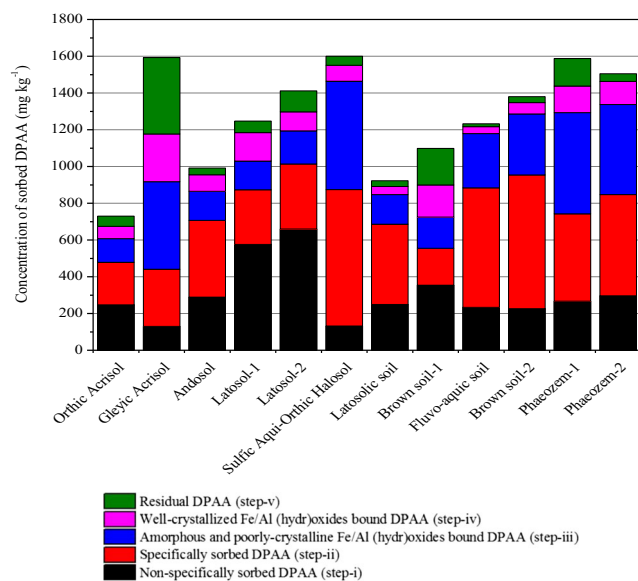


Fig. 1 Sequential extracted concentrations of DPAA in soil clay mineral fractions. Means of each extracted fraction are presented as percentage (%) of the total DPAA (mg kg^{-1}). All results were represented as the mean of two parallels

fractions of eight soils, except for those of Orthic Acrisol soil, Brown soil (30–40%), Latosol-1, and Latosol-2 soils (> 40%), where the values up to 46.7% were found (Fig. 1). This fraction accounts for DPAA bound to the solid surface by electrostatic force and is indicative of out-sphere DPAA complexes. The higher non-specifically fractions from the two Latosol soils might due to their higher contents of $\text{Fe}_2\text{O}_{3\text{DCB}}$ and $\text{Al}_2\text{O}_{3\text{DCB}}$ (Table 1), which are the main sources of positive charge in soils (Goldberg 1989) and might thereby increase DPAA sorption through van der Waals attraction. Significant Pearson's correlation between the non-specifically fraction and $\text{Fe}_2\text{O}_{3\text{DCB}}$ ($p < 0.05$) or $\text{Al}_2\text{O}_{3\text{DCB}}$ ($p < 0.01$) (Table 2) further strengthens this hypothesis.

The specifically fraction (step ii) was the dominant phase and it constituted 18.3–52.8% of the total DPAA (Fig. 1). This fraction represents an estimation of inner-sphere surface complexes (Wenzel et al. 2001) and is useful in providing a relative measure of DPAA that can be potentially mobilized due to changes in pH or phosphate addition (Violante et al. 2010). This result is consistent with the previous study that found DPAA can be effectively desorbed from both Acrisol and Phaeozem soils by addition of phosphate (Wang et al. 2013). Additionally, non-specifically and specifically fractions are likely to constitute the majority of bioaccessible As (Tang et al. 2007). In the case of DPAA, these two fractions constituted more than 46% of the total DPAA in the clay mineral fractions of all soils, except of the Gleyic Acrisol soil (27.7%) (Fig. 1). This proportion is significant higher compared with those previously reported for inorganic As (< 23%) (Taggart et al. 2004; Krysiak and Karczewska 2007), suggesting that DPAA in soil might be more labile and bioaccessible than inorganic As.

The DPAA recovered upon the dissolution of amorphous and poorly crystalline Fe/Al (hydr)oxides (step iii) constituted 15.5–36.9% of the total DPAA in the clay mineral fractions of all soils, except for those of Latosol-1 and Latosol-2 (< 13%) (Fig. 1). For both Latosol soils, higher DPAA fractions were released in the first two steps of the SEP (Fig. 1). This finding may be explained by the higher levels of $\text{Fe}_2\text{O}_{3\text{DCB}}$ versus lower contents of $\text{Fe}_2\text{O}_{3\text{oxalate}}$ (Table 1) for these Latosol soils. The significant correlation of DPAA fractions extracted in the step iii with $\text{Fe}_2\text{O}_{3\text{oxalate}}$ content ($r = 0.669$, $p < 0.05$) (Table 2) further demonstrates this point.

The DPAA released from the dissolution of well-crystallized Fe/Al (hydr)oxides (step iv) decreased considerably compared with that from amorphous and poorly-crystalline Fe/Al (hydr)oxides (step iii), and it constituted less than 17% of the total DPAA (Fig. 1). A relatively strong association of DPAA with amorphous and poorly crystalline Fe (hydr)oxides compared with well-crystallized ones is also supported by the Pearson's correlation (Table 2). Our previous study also found that amorphous ferrihydrite exhibited stronger sorption capacity toward DPAA compared with crystallized goethite and hematite (Zhu et al. 2019). This stronger sorption capacity could be due to the higher specific surface area, and hence sorption site density, of amorphous and poorly crystalline Fe (hydr)oxides (Dixit and Hering 2003).

The DPAA recovered from the dissolution of amorphous, poorly crystalline, and well-crystallized Fe/Al (hydr)oxides in steps iii–iv constituted 20.1–46.2% of the total DPAA (Fig. 1), which is significantly lower compared with values reported for inorganic As (> 50%) (Cancès et al. 2005; Niazi et al. 2011; Marabottini et al. 2013). It can be expected that Fe/Al (hydr)oxides in soil may exhibit lower sorption capacity toward DPAA compared with inorganic As. A similar trend has been observed for DMA (Sarkar et al. 2005; Nagar et al. 2014), in which only 15–25% of the total DMA was found to be associated with Fe/Al (hydr)oxides in soils, even after several months of equilibration. This result might be explained by the steric hindrance from two methyl substituents (Lafferty and Loeffert 2005). Inspection of Table 2 and the correlation matrix demonstrated that DPAA fractions extracted both in the step iii ($r = 0.843$, $p < 0.01$) and in steps iii–iv ($r = 0.698$, $p < 0.05$) were significantly correlated with Q_{ads} . These results provide a means of estimating the DPAA sorption capacity of clay mineral fractions on the basis of DPAA fractions associated with amorphous, poorly crystalline, and well-crystallized Fe/Al (hydr)oxides. It should also be noted that DPAA extracted in steps iii–iv could be a potential source of DPAA contamination during the dissolution of Fe (hydr)oxides in flooded soils (Zhu et al. 2016b). According to our SEP data, a substantial amount of DPAA in the clay mineral fractions from the Gleyic Acrisol soil (46.2%) was presented in this potentially available form (Fig. 1), highlighting the need to consider the potential DPAA release in iron-rich paddy soil.

Table 2 Pearson correlation matrix of DPAA sorption with selected physico-chemical properties of clay mineral fractions ($n = 12$)

	Q_{ads}	$\text{Fe}_2\text{O}_{3\text{oxalate}}$	$\text{Fe}_2\text{O}_{3\text{DCB}}$	Fe_{total}	$\text{Al}_2\text{O}_{3\text{DCB}}$	Al_{total}	pH	PZC	CEC	Si_{total}	Step i	Step ii	Step iii	Step iv	Step v	Steps iii–iv	Steps ii–iv
Q_{ads}	1																
$\text{Fe}_2\text{O}_{3\text{oxalate}}$	0.440	1															
$\text{Fe}_2\text{O}_{3\text{DCB}}$	-0.245	-0.041	1														
Fe_{total}	-0.190	-0.183	0.881**	1													
$\text{Al}_2\text{O}_{3\text{DCB}}$	-0.230	-0.297	0.739**	0.773**	1												
Al_{total}	0.069	-0.347	0.130	0.291	-0.090	1											
pH	0.061	-0.042	0.820**	0.829**	0.746**	0.229	1										
PZC	-0.308	-0.140	0.776**	-0.782**	0.699**	0.122	0.792**	1									
CEC	0.354	0.037	-0.841**	-0.635*	-0.511	0.173	-0.582*	-0.444	1								
Si_{total}	-0.399	0.084	0.172	-0.118	-0.140	-0.366	-0.148	0.091	-0.385	1							
Step i	-0.084	-0.434	0.630*	-0.819**	0.677**	0.335	0.529	0.367	-0.518	0.058	1						
Step ii	0.458	0.467	-0.423	-0.344	-0.533	0.410	-0.255	-0.375	0.566	-0.399	-0.424	1					
Step iii	0.843**	0.669*	-0.502	-0.513	-0.320	-0.236	-0.257	-0.423	0.538	-0.218	0.529	0.572	1				
Step iv	0.452	-0.017	0.059	-0.470	0.419	-0.449	0.248	0.052	-0.127	-0.129	0.042	-0.494	0.290	1			
Step v	0.371	-0.045	-0.085	-0.260	0.113	-0.349	0.081	-0.071	-0.030	-0.041	-0.143	-0.465	0.263	0.891**	1		
Steps iii–iv	0.698*	0.562	-0.478	-0.558	-0.177	-0.531	-0.253	-0.337	0.447	-0.147	-0.582*	0.233	0.901**	0.577**	0.527	1	
Steps ii–iv	0.364	0.545	-0.598*	-0.603*	-0.649*	0.049	-0.428	-0.398	0.643*	-0.233	-0.770*	0.882**	0.691*	-0.354	-0.286	0.482	1

*Significant level at $p < 0.05$ **Significant level at $p < 0.01$

The residual DPAA (step v) was only of minor importance and contributed to less than 10% of the total DPAA in the clay mineral fractions from all soils, except for those of Gleyic Acrisol soil (26.1%) and Brown soil-1 (18.1%) (Fig. 1). This fraction represents As hosted by phyllosilicate and aluminosilicate minerals (Fang and Chen 2015; Kim et al. 2014) and is generally considered as the least mobility for As (Lo and Yang 1998). The highest residual DPAA fraction in the clay mineral fractions of Gleyic Acrisol soil might be explained by its highest concentrations of extracted Al in step v (Fig. S2—ESM), suggesting that more DPAA can reach the interlayers of aluminosilicate.

For all soils, the greatest proportions of added DPAA appeared in steps ii–iv and varied from 45.2 to 88.7% (Fig. 1). Pearson analysis demonstrated that these fractions were significantly correlated with CEC ($r = 0.643$, $p < 0.05$) (Table 2). These results suggest that a major part of DPAA present in these clay mineral fractions would have been, on the one hand, sorbed onto the surface hydroxyl groups at layer silicate edges, onto Fe/Al (hydr)oxides, and onto aluminosilicates via surface complexation, and on the other hand, complexed and/or precipitated embedded inside the Fe/Al (hydr)oxides. The difference is that the former surface interaction causes DPAA to be easily released by specific replacement by phosphate without total dissolution of the mineral particles (Cai et al. 2002).

3.3 Sorption structure of DPAA in clay mineral fractions

The k^3 -weighted EXAFS spectra of DPAA-sorbed samples and their radial distribution functions (RDFs) are displayed in Fig. 2a, b, respectively. Fourier back-transformed k^3 -weighted EXAFS functions of the first, second and third shells are presented in Fig. 3a, b, respectively. Fitting the first, second, and third shells separately (Fig. 3a, b) yielded results similar to those obtained by fitting the whole EXAFS spectra (Fig. 2a, b, Table 3).

All spectra were dominated by the contribution of As-O and As-C₁ (Fig. S1—ESM) mixed in the first shell. The interatomic distances of As-O and As-C₁ were 1.71–1.73 and 1.87–1.91 Å (Table 3), respectively. A broad peak in the RDF at 2.3–3.3 Å was observed in all samples, but was different from that of the DPAA standard (Fig. 3c), the peak was then fitted with As-C₂ (Fig. S1—ESM) and As-Fe pairs. The second-neighbor contribution to the EXAFS spectra was fitted using As-C₂ at various distances. Four C atoms were located at As-C₂ distances of 2.80–2.86 Å (Table 3). The third coordination shell surrounding As was satisfactorily fitted by 1.32–1.51 Fe atoms at As-Fe distances of 3.18–3.25 Å (Fig. 2b, Table 3). These results provide direct evidence that DPAA sorption in clay mineral fractions can mainly be ascribed to the contribution of Fe (hydr)oxides, which agrees with the notion

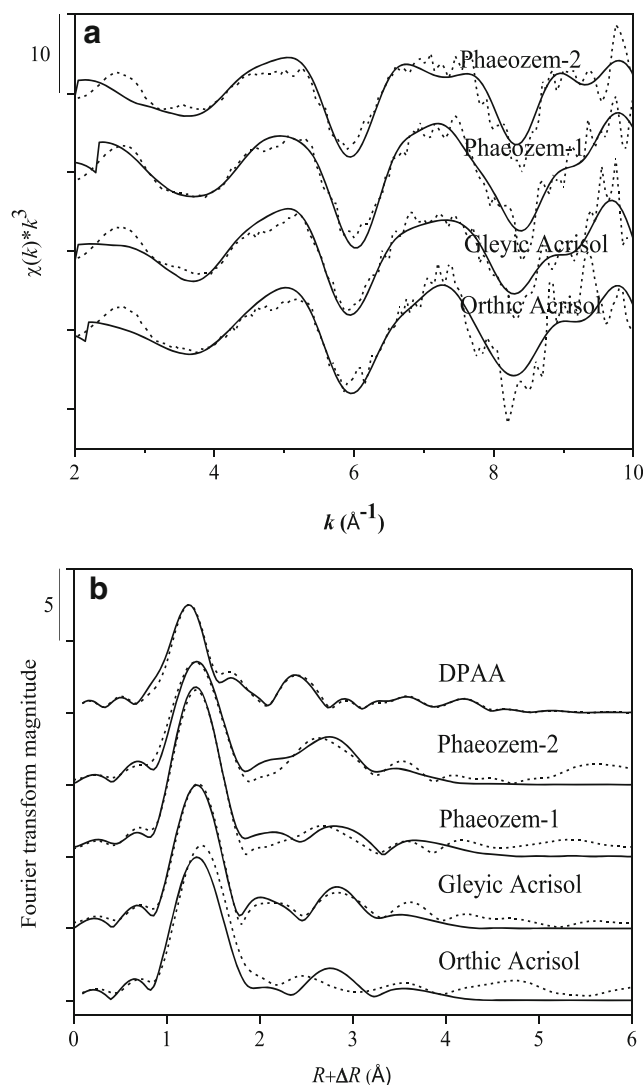


Fig. 2 Normalized k^3 -weighted (a) and Fourier-transformed (b) As-K edge EXAFS spectra for DPAA standard (solid) and DPAA-sorbed clay mineral fractions. Experimental and calculated spectra were displayed as dashed and solid lines, respectively

that DPAA interacts with Fe (hydr)oxides either through surface complexation or through complexation embedded within the Fe (hydr)oxides. Additionally, the fitted As-O, As-C₁, and As-C₂ bond distances from this study are in agreement with previous EXAFS investigations (Tanaka et al. 2014).

Inclusion of another, longer, As-Fe contribution at about 3.5 Å and As-Al contribution did not improve the fit for all samples, and the values of ΔE_0 were unreasonably large when including the additional Fe or Al shell (data not shown). A multiple scattering (MS) As-O-O-As path was also added but did not improve the goodness-of-fit parameters according to the R factors (data not shown). Thus, the MS path was finally not included in all fittings in order to reduce the adjustable variables (Paktunc et al. 2004). The fitted As-Fe distances are in reasonable agreement with previous EXAFS data of inorganic (Beaulieu and Savage 2005) and methyl (Shimizu et al.

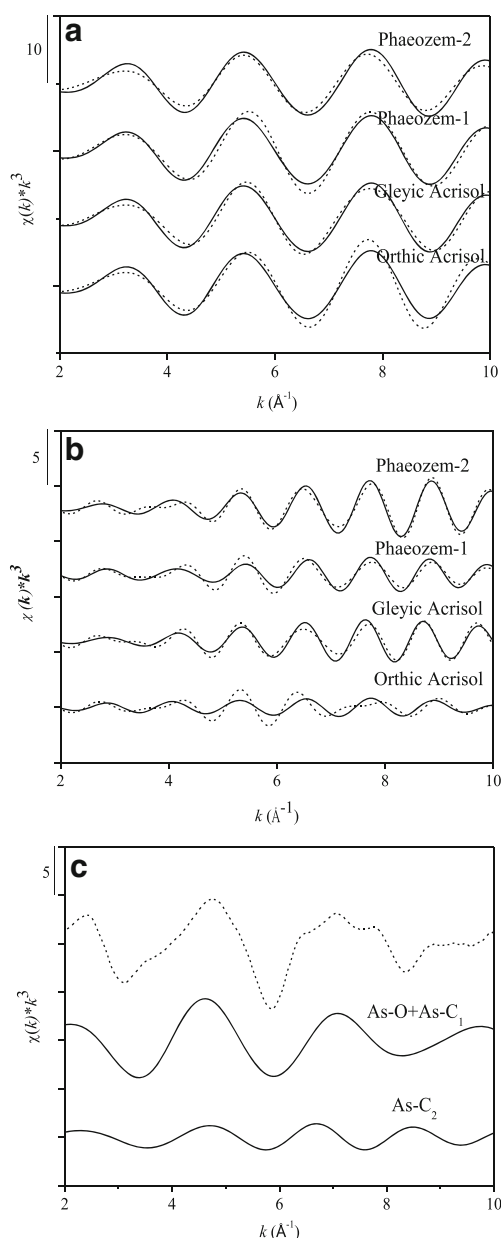


Fig. 3 Partial k^3 -weighted $\chi(k)$ EXAFS functions of first (a), second and third (b) shells for DPAA-sorbed clay mineral fractions, k^3 -weighted EXAFS spectra of DPAA standard (solid) and contributions of first and second shells (c). Fourier back-transformed data were obtained using a Hanning window between 1.1 and 2.3 for the first-shell peak and between 2.3 and 3.7 for the second- and third-shell peaks. Experimental and calculated spectra were displayed as dashed and solid lines, respectively

2011) arsenics, and also correspond well with those of the earlier study, which calculated As-Fe distances of inner-sphere DPAA complexes using density functional theory (DFT) method (Tanaka et al. 2014). It should also be noted that the obtained CNs of As-Fe paths were smaller than 2.0 (Table 3) which indicated that DPAA can form 2C and/or 1V complexes on Fe (hydr)oxides in clay mineral fractions.

Possible inner-sphere complexes of As formed on Fe (hydr)oxides can be classified into 1V , 2C , and bidentate

monuclear edge-sharing (2E) (Fendorf et al. 1997). A shorter As-Fe distance (2.8–3.0 Å) corresponded to a controversial 2E structure which has been argued to be energetically unstable and usually misinterpreted (Sherman and Randall 2003). This shorter As-Fe distance was absent in the present study. The fitted As-Fe distances of 3.18–3.25 Å are too close for As-Fe 1V complexes, which is 3.46 Å based on EXAFS studies and 3.52 Å based on DFT calculations (Tanaka et al. 2014). This longer As-Fe distance (3.5–3.6 Å) was also found to be absent in DPAA-sorbed clay mineral fractions but has been found to contribute significantly for DPAA sorption on ferrihydrite (Tanaka et al. 2014). There is a possibility that the signal of longer As-Fe path at distances of 3.5–3.6 Å might be masked by the dominance of As-Fe path at distances of 1.32–1.51 Å (Waychunas et al. 1993) due to the low signal-to-noise ratio in the measured spectra. Therefore, despite of no evidence of DPAA 1V complexes, it was impossible to exclude them based on the present study. Considering the different crystal structure of Fe (hydr)oxides, and the complicated environmental conditions in clay mineral fractions, different types of inner-sphere DPAA complexes may form. Additionally, the EXAFS technique used in this study cannot verify out-sphere complex formation (Catalano et al. 2008); however, the combination of SEP and EXAFS techniques together demonstrates the simultaneous formation of inner-sphere and out-sphere complexes for DPAA sorption on clay mineral fractions.

3.4 Comparison with previous studies for methyl and phenyl arsenics

It is well-recognized that increased methyl substitution results in decreased As sorption by Fe (hydr)oxides (Zhang et al. 2007). This can be explained by the following reasons: (i) the number of hydroxyl groups available for complexation decreases with increasing methyl group substitution, and the larger size of the methyl group compared with the hydroxyl group could increase steric hindrance (Lafferty and Loeppert 2005) and hence weaken Fe-O-As bonds; (ii) the steric hindrance caused by methyl group could make neighboring sites on Fe (hydr)oxides inaccessible for further complexation (Adamescu et al. 2010), thus decreasing the availability of hydroxyl groups. Similarly, the formation of inner-sphere complexes could also put stress on the geometry of DPAA, the steric hindrance may thereby make DPAA/Fe complexes unstable, and the number of DPAA molecules/ions that can sorb to Fe (hydr)oxides is reduced. This effect may explain why a substantial amount of DPAA in clay mineral fractions existed as labile forms (Fig. 1) and the reduced Pearson correlation between Q_{ads} and Fe_{total} , $Fe_2O_{3\text{oxalate}}$, or $Fe_2O_{3\text{DCB}}$ (Table 2).

Group substitution could also affect the complexation environment of organoarsenic. Our EXAFS results demonstrate

Table 3 Summary of As shell-by-shell fitting results for DPAA-sorbed clay mineral fractions

Sample	Ligand	CN	R (Å)	ΔE_0 (eV)	σ^2 (Å ²)	R factor
DPAA standard	As-O	2.00	1.70 (± 0.02)	8.10	0.0030	0.009
	As-C ₁	2.00	1.99 (± 0.03)	–	0.0010	
	As-C ₂	4.00	2.87 (± 0.06)	–	0.0010	
Orthic Acrisol	As-O	2.00	1.73 (± 0.06)	– 10.18	0.0030	0.041
	As-Fe	1.44 (± 0.27)	3.25 (± 0.13)	–	0.0030	
	As-C ₁	2.00	1.91 (± 0.22)	–	0.0030	
	As-C ₂	4.00	2.81 (± 0.22)	–	0.0030	
Gleyic Acrisol	As-O	2.00	1.71 (± 0.02)	3.92	0.0017	0.022
	As-Fe	1.51 (± 0.45)	3.24 (± 0.10)	–	0.0030	
	As-C ₁	2.00	1.91 (± 0.17)	–	0.0030	
	As-C ₂	4.00	2.84 (± 0.17)	–	0.0030	
Phaeozem-1	As-O	2.00	1.73 (± 0.05)	5.32	0.0010	0.013
	As-Fe	1.36 (± 0.47)	3.19 (± 0.14)	–	0.0030	
	As-C ₁	2.00	1.87 (± 0.16)	–	0.0030	
	As-C ₂	4.00	2.86 (± 0.16)	–	0.0030	
Phaeozem-2	As-O	2.00	1.71 (± 0.03)	15.26	0.0011	0.035
	As-Fe	1.32 (± 1.07)	3.18 (± 0.16)	–	0.0030	
	As-C ₁	2.00	1.89 (± 0.13)	–	0.0030	
	As-C ₂	4.00	2.80 (± 0.13)	–	0.0030	

All parameter values indicated by (–) were linked to the parameter value placed above in the table. Numbers in parentheses represent deviations. CN values for As-O, As-C₁, and As-C₂ were fixed to theoretical values. As-C₁ and As-C₂ paths shared one σ^2 during the fitting process

the formation of DPAA ²C and/or ¹V complexes on clay mineral fractions. Such inner-sphere bonds are partly coincident with our previous observation for DPAA ²C complexes on ferrihydrite, goethite, and hematite, and partly coincident with those observed by Tanaka et al. (2014), who found both DPAA ²C and ¹V complexes on ferrihydrite. The discrepancy may lie on the different surface coverage of As on Fe (hydr)oxides (Fendorf et al. 1997). It was suggested that DPAA ²C complexes may be favored at low surface coverage, while both ²C and ¹V complexes are at a relatively high surface coverage, with the formation of the ¹V complexes possibly conserving the sorption site. Similar phenomena can be discerned for DMA sorption on Fe (hydr)oxides according to the results from Shimizu et al. (2011) and Tanaka et al. (2013). However, for *p*AsA, only the ¹V bond was found to be prevalent on Fe (hydr)oxides (Chabot et al. 2009; Adamescu et al. 2014). This result can be explained partly by the steric effect derived from the substituents (Depalma et al. 2008), and also by the charge balance resulting from the resonance between uncomplexed As=O and As-OH groups when formed ¹V bond (Arts et al. 2013). However, the charge balance for DMA cannot be achieved in the same way due to its increased organic substituents. On the other hand, the steric hindrance makes two methyl substituents difficult to move closer to fulfill the charge imbalance of As⁺-O⁻ bond when forms ²C complexes, the remaining O atom therefore has to move closer to As atom, which may contribute to the formation of DMA ²C complexes (Shimizu et al. 2010). According to these

results, similar ²C and ¹V complexes can be expected for DPAA due to its similar molecular structure with *p*AsA and DMA. More experimental data and theory calculations are still needed to investigate which types of inner-sphere DPAA complexes are more favorable on various solid surfaces found in the soil-water environment.

3.5 Environmental relevancy of the findings

The current study reveals that DPAA concentrations of labile fractions including non-specifically and specifically ones are of particular concern as they occupy substantial parts of the total DPAA in clay mineral fractions, and that natural attenuation might be inadequate to control the mobility and thereby bioaccessibility of DPAA in soils. A substantial amount of DPAA was also associated with amorphous, poorly-crystalline and well-crystallized Fe/Al (hydr)oxides. Pearson's correlation analysis and EXAFS results further indicate that the formation of inner-sphere DPAA complexes on Fe (hydr)oxides, especially amorphous and poorly crystalline ones, contributes most to DPAA sorption in clay mineral fractions. This observation suggests that the speciation of Fe (hydr)oxides should be considered when predicting the fate, mobility, and bioaccessibility of DPAA in the soil-water environment, especially in paddy soil where the transformation of Fe mineralogy always accompanies the mobilization of As (Yamaguchi et al. 2011).

4 Conclusions

This study investigated the speciation and sorption structure of DPAA in soil clay mineral fractions. The results showed that DPAA in clay mineral fractions predominantly existed as specifically, amorphous, poorly crystalline and well-crystallized Fe/Al (hydr)oxides associated fractions, and amorphous/poorly crystalline Fe rather than total Fe contributed more to DPAA sorption. EXAFS data provided direct evidence that DPAA formed inner-sphere complexes on Fe (hydr)oxides. A combination of SEP and EXAFS results demonstrated that DPAA interacted with clay mineral fractions via (1) electrostatic attraction; (2) surface complexation, mainly on Fe (hydr)oxides; (3) complexation embedded inside the Fe (hydr)oxides; and (4) reaching the interlayers of aluminosilicate. It was suggested that the steric hindrance caused by phenyl substitution can, on the one hand, make DPAA/Fe complexes unstable and decrease the number of sorbed DPAA molecules/ions, and on the other hand, change the way the central As atom maintains its charge balance. This may explain why a certain amount of DPAA in clay mineral fractions still presented as weakly bound forms and the formation of DPAA ^{235}C and/or ^{235}V complexes, respectively.

Acknowledgments We are thankful to Dr. Xu Wang for his technical assistance during the experiments at SSRF and Dr. Junqing Xu for his useful suggestion during the data analysis at the National Synchrotron Radiation Laboratory (NSRL), University of Science and Technology of China. We would also like to thank Dr. Xueli Wu for the help in HPLC-MS/MS analysis.

Funding information This study received financial support from the National Natural Science Foundation of China (no. 41807117 and 41230858), the Key Projects of Natural Science Research of Universities in Anhui Province (no. KJ2018A0315), the Doctoral Research Start-up Funds Project of Anhui Normal University (no. 2018XJJ50), the Talent Cultivation Project of Anhui Normal University (no. 2018XJJ82), and the Cultivation Project on Excellent Undergraduates' Thesis (design, create) of Anhui Normal University (no. pyjh2018487).

References

- Adamescu A, Mitchell W, Hamilton IP, Al-Abadleh HA (2010) Insights into the surface complexation of dimethylarsinic acid on iron (oxyhydr) oxides from ATR-FTIR studies and quantum chemical calculations. *Environ Sci Technol* 44:7802–7807
- Adamescu A, Hamilton IP, Al-Abadleh HA (2014) Density functional theory calculations on the complexation of *p*-Arsanilic acid with hydrated iron oxide clusters: structures, reaction energies, and transition states. *J Phys Chem A* 118:5667–5679
- Arao T, Maejima Y, Baba K (2009) Uptake of aromatic arsenicals from soil contaminated with diphenylarsinic acid by rice. *Environ Sci Technol* 43:1097–1101
- Arčon I, van Elteren JT, Glass HJ, Kodre A, Šlejkovec Z (2005) EXAFS and XANES study of arsenic in contaminated soil. *X-Ray Spectrom* 34:435–438
- Arroyo-Abad U, Elizalde-González MP, Hidalgo-Moreno CM, Mattusch J, Wennrich R (2011) Retention of phenylarsenicals in soils derived from volcanic materials. *J Hazard Mater* 186:1328–1334
- Arts D, Abdus Sabur M, Al-Abadleh HA (2013) Surface interactions of aromatic organoarsenical compounds with hematite nanoparticles using ATR-FTIR: kinetic studies. *J Phys Chem A* 117:2195–2204
- Bacon JR, Davidson CM (2008) Is there a future for sequential chemical extraction? *Analyst* 133:25–46
- Beaulieu BT, Savage KS (2005) Arsenate adsorption structures on aluminum oxide and phyllosilicate mineral surfaces in smelter-impacted soils. *Environ Sci Technol* 39:3571–3579
- Cai Y, Cabrera JC, Georgiadis M, Jayachandran L (2002) Assessment of arsenic mobility in the soils of some golf courses in South Florida. *Sci Total Environ* 291:123–134
- Cancès B, Juillot F, Morin G, Laperche V, Alvarez L, Proux O, Hazemann JL, Brown GE Jr, Calas G (2005) XAS evidence of As(V) association with iron oxyhydroxides in a contaminated soil at a former arsenical pesticide processing plant. *Environ Sci Technol* 39:9398–9405
- Catalano JG, Park C, Fenter P, Zhang Z (2008) Simultaneous inner- and outer-sphere arsenate adsorption on corundum and hematite. *Geochim Cosmochim Acta* 72:1986–2004
- Chabot M, Hoang T, Al-Abadleh HA (2009) ATR-FTIR studies on the nature of surface complexes and desorption efficiency of *p*-arsanilic acid on iron (oxyhydr)oxides. *Environ Sci Technol* 43:3142–3147
- Daus B, Hempel M, Wennrich R, Weiss H (2010) Concentrations and speciation of arsenic in groundwater polluted by warfare agents. *Environ Pollut* 158:3439–3444
- Deng HM, Evans POM (1997) Social and environmental aspects of abandoned chemical weapons in China. *Nonproliferat Rev* 4:101–108
- Depalma S, Cowen S, Hoang T, Al-Abadleh HA (2008) Adsorption thermodynamics of *p*-arsanilic acid on iron (oxyhydr) oxides: in-situ ATR-FTIR studies. *Environ Sci Technol* 42:1922–1927
- Dixit S, Hering JG (2003) Comparison of arsenic(V) and arsenic(III) sorption onto iron oxide minerals: implications for arsenic mobility. *Environ Sci Technol* 37:4182–4189
- Fang TH, Chen YS (2015) Arsenic speciation and diffusion flux in Danshuei Estuary sediments, northern Taiwan. *Mar Pollut Bull* 101:98–109
- Fendorf S, Eick MJ, Grossl P (1997) Arsenate and chromate retention mechanisms on goethite. 1. Surface structure. *Environ Sci Technol* 31:315–320
- Fu QL, Liu C, Achal V, Wang YJ, Zhou DM (2016) Aromatic arsenical additives (AAAs) in the soil environment: detection, environmental behaviors, toxicities, and remediation. *Adv Agron* 140:1–41
- Garnaga G, Wyse E, Azemard S, Stankevičius A, de Mora S (2006) Arsenic in sediments from the southeastern Baltic Sea. *Environ Pollut* 144:855–861
- GB/T22105. 2 (2008) Soil quality-analysis of total mercury, arsenic and lead contents in soils-atomic fluorescence spectrometry-part 2: analysis of total arsenic contents in soils. State Environmental Protection Administration of China
- Girouard E, Zagury GJ (2009) Arsenic bioaccessibility in CCA-contaminated soils: influence of soil properties, arsenic fractionation, and particle-size fraction. *Sci Total Environ* 407:2576–2585
- Goldberg S (1989) Interaction of aluminum and iron oxides and clay minerals and their effect on soil physical properties: a review. *Commun Soil Sci Plan* 20:1181–1207
- Gong ZT (2007) *Pedogenesis and soil taxonomy*. Science Press, Beijing (in Chinese)

- Hanaoka S, Nomura K, Kudo S (2005a) Identification and quantitative determination of diphenylarsenic compounds in abandoned toxic smoke canisters. *J Chromatogr A* 1085:213–223
- Hanaoka S, Nagasawa E, Nomura K, Yamazawa M, Ishizaki M (2005b) Determination of diphenylarsenic compounds related to abandoned chemical warfare agents in environmental samples. *Appl Organomet Chem* 19:265–275
- Hempel M, Daus B, Vogt C, Weiss H (2009) Natural attenuation potential of phenylarsenicals in anoxic groundwaters. *Environ Sci Technol* 43:6989–6995
- Jackson ML (1975) Soil chemical analysis. University of Wisconsin, Madison
- Kelly SD, Hesterberg D, Ravel B (2008) Analysis of soils and minerals using X-ray absorption spectroscopy. In: Ulery AL, Drees R (eds) Methods of soil analysis, part 5, Mineralogical Methods. SSSA, Madison, p 444
- Kim EJ, Yoo JC, Baek K (2014) Arsenic speciation and bioaccessibility in arsenic-contaminated soils: sequential extraction and mineralogical investigation. *Environ Pollut* 186:29–35
- Krysiak A, Karczewska A (2007) Arsenic extractability in soils in the areas of former arsenic mining and smelting, SW Poland. *Sci Total Environ* 379:190–200
- Lafferty BJ, Loeppert RH (2005) Methyl arsenic adsorption and desorption behavior on iron oxides. *Environ Sci Technol* 39:2120–2127
- Lo IMC, Yang XY (1998) Removal and redistribution of metals from contaminated soils by a sequential extraction method. *Waste Manag* 18:1–7
- Lombi E, Sletten RS, Wenzel WW (2000) Sequential arsenic extracted from different size fractions of contaminated soils. *Water Air Soil Pollut* 124:319–332
- Lu RK (2000) Soil and agricultural chemical analysis methods. Chinese Agricultural Science and Technology, Beijing (in Chinese)
- Maejima Y, Murano H, Iwafune T, Arai T, Baba K (2011) Adsorption and mobility of aromatic arsenicals in Japanese agricultural soils. *Soil Sci Plant Nutr* 57:429–435
- Manful G (1992) Occurrence and ecochemical behaviour of arsenic in a goldsmelter impacted area in Ghana. Dissertation, Centrum voor milieusaneringen aan de RUG
- Marabottini R, Stazi SR, Papp R, Grego S, Moscatelli MC (2013) Mobility and distribution of arsenic in contaminated mine soils and its effects on the microbial pool. *Ecotoxicol Environ Saf* 96:147–153
- Nagar R, Sarkar D, Makris KC, Datta R (2014) Arsenic bioaccessibility and speciation in the soils amended with organoarsenicals and drinking-water treatment residuals based on a long-term greenhouse study. *J Hydrol* 518:477–485
- Newville M (2001) IFEFFIT: interactive XAFS analysis and FEFF fitting. *J Synchrotron Radiat* 8:322–324
- Niazi NK, Singh B, Shah P (2011) Arsenic speciation and phytoavailability in contaminated soils using a sequential extraction procedure and XANES spectroscopy. *Environ Sci Technol* 45:7135–7142
- Ochi T, Suzuki T, Isono H, Kaise T (2004) In vitro cytotoxic and genotoxic effects of diphenylarsinic acid, a degradation product of chemical warfare agents. *Toxicol Appl Pharm* 200:64–72
- Paktunc D, Foster A, Heald S, Laflamme G (2004) Speciation and characterization of arsenic in gold ores and cyanidation tailings using X-ray absorption spectroscopy. *Geochim Cosmochim Acta* 68:969–983
- Palumbo-Roe B, Wragg J, Cave M (2015) Linking selective chemical extraction of iron oxyhydroxides to arsenic bioaccessibility in soil. *Environ Pollut* 207:256–265
- Pretorius W, Weis D, Williams G, Hanano D, Kieffer B, Scoates J (2006) Complete trace elemental characterisation of granitoid (USGS G-2, GSP-2) reference materials by high resolution inductively coupled plasma-mass spectrometry. *Geostand Geoanal Res* 30:39–54
- Sakurai K, Ohdate Y, Kyuma K (1988) Comparison of salt titration and potentiometric titration methods for the determination of zero point of charge (ZPC). *Soil Sci Plant Nutr* 34:171–182
- Sarkar D, Datta R, Sharma S (2005) Fate and bioavailability of arsenic in organo-arsenical pesticide-applied soils: part-I: incubation study. *Chemosphere* 6:188–195
- Sherman DM, Randall SR (2003) Surface complexation of arsenic(V) to iron(III) (hydr)oxides: structural mechanism from ab initio molecular geometries and EXAFS spectroscopy. *Geochim Cosmochim Acta* 67:4223–4230
- Shimizu M, Ginder-Vogel M, Parikh SJ, Sparks DL (2010) Molecular scale assessment of methylarsenic sorption on aluminum oxide. *Environ Sci Technol* 44:612–617
- Shimizu M, Arai Y, Sparks DL (2011) Multiscale assessment of methylarsenic reactivity in soil. 1. Sorption and desorption on soils. *Environ Sci Technol* 45:4293–4299
- Taggart MA, Carlisle M, Pain DJ, Williams R, Osborn D, Joyson A, Meharg AA (2004) The distribution of arsenic in soils affected by the Aznalcóllar mine spill, SW Spain. *Sci Total Environ* 323:137–152
- Tanaka M, Takahashi Y, Yamaguchi N (2013) A study on adsorption mechanism of organoarsenic compounds on ferrihydrite by XAFS. *J Phys Conf Ser* 430:012100
- Tanaka M, Togo YS, Yamaguchi N, Takahashi Y (2014) An EXAFS study on the adsorption structure of phenyl-substituted organoarsenic compounds on ferrihydrite. *J Colloid Interf Sci* 415:13–17
- Tang XY, Zhu YG, Shan XQ, McLaren R, Duan J (2007) The ageing effect on the bioaccessibility and fractionation of arsenic in soils from China. *Chemosphere* 66:1183–1190
- van Herreweghe S, Swennen R, Vandecasteele C, Cappuyns V (2003) Solid phase speciation of arsenic by sequential extraction in standard reference materials and industrially contaminated soil samples. *Environ Pollut* 122:323–342
- Violante A, Cozzolino V, Perelomov L, Caporale AG, Pigna M (2010) Mobility and bioavailability of heavy metals and metalloids in soil environments. *J Soil Sci Plant Nutr* 10:268–292
- Wang S, Mulligan CN (2008) Speciation and surface structure of inorganic arsenic in solid phases: a review. *Environ Int* 34:867–879
- Wang AN, Li SY, Teng Y, Liu WX, Wu LH, Zhang HB, Huang YJ, Luo YM, Christie P (2013) Adsorption and desorption characteristics of diphenylarsenicals in two contrasting soils. *J Environ Sci* 25:1172–1179
- Wang YN, Zeng XB, Lu YH, Su SM, Bai LY, Li LF, Wu CX (2015) Effect of aging on the bioavailability and fractionation of arsenic in soils derived from five parent materials in a red soil region of Southern China. *Environ Pollut* 207:79–87
- Waychunas GA, Rea BA, Fuller CC, Davis JA (1993) Surface chemistry of ferrihydrite: part 1. EXAFS studies of the geometry of coprecipitated and adsorbed arsenate. *Geochim Cosmochim Acta* 57:2251–2269
- Wenzel WW, Kirchnerbaumer N, Prohaska T, Stingseder G, Lombi E, Adriano DC (2001) Arsenic fractionation in soils using an improved sequential extraction procedure. *Anal Chim Acta* 436:309–323
- Yamaguchi N, Nakamura T, Dong F, Takahashi Y, Amachi S, Makino T (2011) Arsenic release from flooded paddy soils is influenced by speciation, Eh, pH, and iron dissolution. *Chemosphere* 83:925–932
- Zhang GL, Gong ZT (2012) Soil survey laboratory methods. Science Press, Beijing (in Chinese)
- Zhang JS, Stanforth RS, Pehkonen SO (2007) Effect of replacing a hydroxyl group with a methyl group on arsenic(V) species adsorption on goethite (α -FeOOH). *J Colloid Interface Sci* 306:16–21

- Zhu M, Tu C, Zhang HB, Luo YM, Christie P (2016a) Simultaneous determination of diphenylarsinic and phenylarsinic acids in amended soils by optimized solvent extraction coupled to HPLC-MS/MS. *Geoderma* 270:109–116
- Zhu M, Tu C, Hu XF, Zhang HB, Zhang LJ, Wei J, Li Y, Luo YM, Christie P (2016b) Solid-solution partitioning and thionation of diphenylarsinic acid in a flooded soil under the impact of sulfate and iron reduction. *Sci Total Environ* 569:1579–1586
- Zhu M, Hu XF, Tu C, Zhang HB, Song F, Luo YM, Christie P (2019) Sorption mechanisms of diphenylarsinic acid on ferrihydrite, goethite and hematite using sequential extraction, FTIR measurement and XAFS spectroscopy. *Sci Total Environ* 669:991–1000

Publisher's note Springer Nature remains neutral with regard to jurisdictional claims in published maps and institutional affiliations.